Prediction of superconductivity at 70 K in a pristine monolayer of LiBC

P. Modak,[1,2,*] Ashok K. Verma,[1,†] and Ajay K. Mishra[1,2]

[1]*High Pressure & Synchrotron Radiation Physics Division, Bhabha Atomic Research Centre, Mumbai 400085, India*

[2]*Homi Bhabha National Institute, Mumbai 400094, India*

(Received 11 January 2021; revised 10 May 2021; accepted 21 July 2021; published 6 August 2021)

Search of high-temperature superconductors has gained huge impetus since the discovery of superconductivity in bulk MgB_2. These efforts led to the synthesis of high-T_C materials in the megabar pressure region. However, the ultimate goal of a room-conditions superconductor is still elusive. Toward this, a class of two-dimensional (2D) superconductors is emerging as a fertile field of research. In this paper, by solving fully anisotropic Migdal-Eliashberg equations, we show that a pristine monolayer (ML) of LiBC will be a Bardeen-Cooper-Schrieffer-type superconductor with a record-breaking T_C of 70 K among pure 2D superconductors. The critical temperature could be further increased by hydrogenation of the ML. Analysis of the electronic properties indicates the partial change of B-C covalent bonding from sp^2 to sp^3 type on bulk-to-ML transformation. This paper presents a proposal to metalize the LiBC system, which was long been predicted to show superconductivity in its bulk form with 50% Li site vacancies. This system might be useful for the design and development of high-T_C 2D superconductors that could be applied in devices like quantum interferometers, superconducting qubits, or superconducting transistors.

DOI: 10.1103/PhysRevB.104.054504

Superconductivity—the phenomenon of sans resistance flow of conduction electrons—remains one of the hot topics in material science even after a century of its discovery [1]. Since the beginning, it was realized that the occurrence of this electronic property at room-conditions could make a paradigm shift in technological innovations. However, this did not materialize mainly due to the lack of thorough understanding of high-T_C superconductivity in cuprates [2–4] and the low critical temperature of conventional [Bardeen-Cooper-Schrieffer (BCS) type] superconductors [5,6]. Naturally, huge efforts have been devoted to understanding high-T_C cuprates and related materials while overlooking the BCS superconductors. However, discovery of BCS-type superconductivity at 39 K in bulk MgB_2 [7] shifted attention from the high-T_C copper oxide family to the BCS-type superconductors. Lately, exploration of high-T_C superconductors outside the high-T_C cuprates became one of the most vibrant fields of research in material science. Due to these efforts, recently, many hydrogen-rich materials like SH_3, LaH_{10}, or carbonaceous-sulfur hydride were synthesized at megabar pressures with $T_C > 200$ K [8–10]. Such studies have clearly established that high-T_C superconductivity is achievable in a BCS-type superconductor analogous to solid hydrogen [11].

Material properties like high vibrational energy scale, strong electron-phonon coupling (EPC), and large electronic density of states (DOS) at the Fermi level (N_{E_F}) are primary requirements for a material to be a high-T_C BCS-type superconductor. Bulk LiBC is one such system isostructural to MgB_2 that could easily satisfy these criteria, as it consists of lighter Li atoms and possesses strong B-C covalent bonds. Earlier theoretical studies [12–14] have shown that bulk LiBC is an insulator with covalent bonding states lying at the top of the valence bands. A possible superconducting state could be realized in bulk LiBC by elevating σ-bonding states above the Fermi level by means of doping, pressure, alloying, etc. [14–19]. It is expected that the electronic and superconducting properties of engineered LiBC would be like that of MgB_2. The coupling between σ-bonding electrons and bond-stretching phonons is also expected to be strong. Indeed hole-doped bulk Li_xBC ($x = 0.5$) is a system of the LiBC family which was predicted to exhibit superconductivity at ~100 K [14]. However, 50% Li vacancies destabilize the crystal lattice, and so the synthesis of hole-doped samples becomes impractical in laboratories [20]. The high-pressure route of metallization has also not succeeded [21,22]. Therefore, metallization of pristine LiBC is itself a challenging problem.

Here, in this paper, using density functional theory-based calculations, we show that reduction of dimension drives the insulating bulk LiBC to a metal. On dimension reduction from bulk to the monolayer (ML) form, bonding in B-C honeycomb changes from sp^2 to partial sp^3 type. However, the hybridization of σ-bonding states with other conduction states is small enough to retain the original σ-bonding characteristics. Consequently, ML-LiBC shows superconductivity with $T_C \approx 70$ K that further increases on hydrogenation. It is to be noted here that our results are for pristine ML-LiBC in contrast with other materials such as transition metal dichalcogenides and doped graphene, etc., where superconductivity is observed in the modified ML form [23–25]. These modifications could be either a specific substrate, an intercalant atom, or a particular type of dopant atom which plays a crucial role in their superconductivity. Unlike bulk LiBC, MgB_2 exhibits superconductivity in its bulk form; therefore, it is very likely

*pmodak@barc.gov.in, paritoshmodak295@gmail.com

†hpps@barc.gov.in

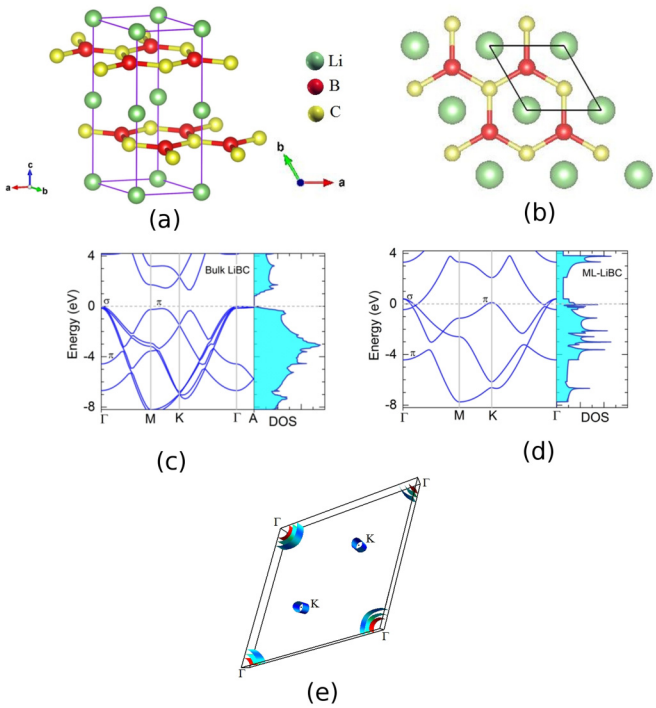

FIG. 1. (a) and (b) Crystal structures. (c) and (d) Electronic band structure and density of states (DOS; in units of states/eV/cell) of bulk LiBC and ML-LiBC, respectively. (e) Fermi surface of ML-LiBC.

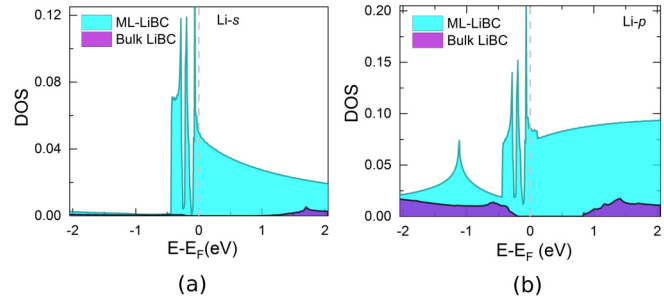

FIG. 2. Partial Li density of states (DOS) both for bulk LiBC and ML-LiBC. Here, DOS is expressed in units of states/eV/atom: (a) *s* type, (b) *p* type.

that its pristine ML will also show superconductivity, as predicted in Ref. [26].

Notably, over five decades ago, the very existence of two-dimensional (2D) materials was uncertain because of the Hohenberg-Mermin-Wagner theorem, which prohibits long-range ordering in materials for dimensions $D \leqslant 2$ at finite temperatures [27,28]. However, recent innovations in fabrication technology have led to production of a large number of 2D materials [29], and thus, the field of 2D superconductors has also evolved into a very fertile area of research with several possible applications in devices like quantum interferometers, superconducting qubits, or superconducting transistors [30]. ML-LiBC could be prepared from the LiBC crystals by using a mechanical exfoliation technique [31] that has been used in the past for extraction of 2D sheets of various layered inorganic materials such as MoS_2 or WS_2.

Bulk LiBC has a layered hexagonal structure (space group P6/*mmm*) that consists of alternate B-C honeycomb layers separated by a layer of interstitial Li atoms [32] [see Fig. 1(a)]. To prepare the simulation cell, we took one hexagonal BC layer attached with Li atoms on one side, whereas a vacuum layer of 15 Å width was inserted on the other side to avoid unphysical interactions with its periodic image [Fig. 1(b)]. All cell optimizations and electronic structure calculations were carried out using the *ab initio* plane-wave pseudopotential method as implemented in the QUANTUM ESPRESSO package [33]. We used norm-conserving von Barth–Car pseudopotentials with 100 Ry plane-wave energy cutoff and local density approximation for the exchange correlations. For Brillouin zone (BZ) sampling, we used Γ-centered uniform $25\times25\times10$ and $40\times40\times1$ k-point meshes for bulk LiBC and its ML, respectively. To study effects of spin-orbit (SO) coupling interactions, we used fully relativistic pseudopotentials.

Our optimized lattice parameters for bulk LiBC ($a = 2.705$ Å and $c = 6.977$ Å) compare well with that of the experimental data ($a = 2.752$ Å and $c = 7.058$ Å) [32]. For the ML, the in-plane lattice constant $a = 2.708$ Å is slightly bigger than the bulk. Figures 1(c) and 1(d) represent electronic band structure and DOS of bulk and ML-LiBC, respectively. Electronic bands corresponding to the σ and π-bonding orbitals of B and C atoms lead to hole pockets around Γ and K points, respectively. Interestingly, another rather dispersive band resulting from the hybridization of Li s states and π^* states of B and C atoms intersects the Fermi level close to the Γ point. These three partially occupied bands form four Fermi sheets, three around the Γ point and one around the K point, as shown in Fig. 1(e).

To understand the insulator-to-metal transition on dimension reduction, we compared l-projected DOS functions of Li atoms for both bulk and the ML (Fig. 2). For the ML, it indicates a smaller charge transfer from the Li s state to the graphitic BC layer, as s DOS near E_F has substantial weight, whereas in the case of the bulk, there is nearly complete transfer of the Li s charge, as it has negligible s DOS. Higher Li p partial DOS close to E_F in the ML is due to the hybridization of Li s and B-C π^* states. To gain further insight, we carried out tight-binding Slater-Koster-type parameter fitting of the *ab initio* electronic band structures for the bulk and the ML [34]. For ML-LiBC, we notice that only s and p states of B and C atoms and the s state of the Li atom are sufficient to reproduce the *ab initio* band structure accurately. In contrast, for bulk LiBC, an additional Li p state is also needed. Interestingly, for ML-LiBC, only $sp\sigma$-type hopping elements have finite values for Li-B and Li-C interactions, while in the case of bulk LiBC, all $sp\sigma$-, $pp\sigma$-, and $pp\pi$-type hopping elements have finite values. These findings imply that electrons can easily hop from the Li atom to the BC plane in the bulk because of availability of extra hopping channels, making the system an insulator. Indeed, Bader charge analysis [35] shows ∼7% higher charge transfer from the Li atom to the BC plane ($0.85e^-$ for bulk and $0.79e^-$ for the ML) in bulk LiBC. This indicates a greater ionic character for the Li-B and Li-C interactions in bulk.

The calculated hopping parameters of the B-C interactions (Table I) show that the hopping integrals between p_x and p_y orbitals of one type of atom to the p_z orbital of other types

TABLE I. Hopping matrix elements (in eV) of B-C interactions in the bulk and ML-LiBC.

	B			
C	s	p_x	p_y	p_z
Bulk LiBC: interaction: B-C (bond length = 1.59 Å)				
s	4.139	−2.327	4.030	0.000
p_x	2.327	0.230	2.527	0.000
p_y	−4.030	2.527	−2.688	0.000
p_z	0.000	0.000	0.000	1.689
ML-LiBC: interaction: B-C (bond length = 1.59 Å)				
s	3.915	−3.163	1.826	0.215
p_x	3.163	−1.022	1.463	0.172
p_y	−1.826	1.463	0.668	−0.100
p_z	−0.215	0.172	−0.100	1.501

of atoms are zero for the bulk LiBC, whereas these integrals have finite values for ML-LiBC, indicating that p_x and p_y orbitals are orthogonal to the p_z orbital in the bulk but not in the ML. Thus, B-C interactions in ML-LiBC involve partial sp^3-type hybridization, unlike pure sp^2-type hybridization in bulk. Furthermore, Wannier function constructions show that ML-LiBC needs one Li atom-centered function, whereas bulk LiBC does not need this function, indicating a complete transfer of Li s electrons to graphitic p states in the bulk.

The electronic band structure of ML-LiBC, especially the bonding σ bands close to E_F, appears quite like the MgB_2 [36]. Because of a sharp peak close to E_F, it has higher DOS than MgB_2 at E_F ($N_{E_F} \approx 0.8$ states/eV/f.u. for ML-LiBC and $N_{E_F} \approx 0.7$ states/eV/f.u. for MgB_2). Higher N_{E_F} values are essential for achieving a high-T_C superconductivity in addition to a strong EPC that could exist between σ electrons and zone-centered in-plane bond-stretching phonons in the case of ML-LiBC.

To calculate phonon properties and electron-phonon interactions, we used density functional perturbation theory [37]. By calculating the electronic spectra, phonon spectra, and their interactions, we solved fully anisotropic Migdal-Eliashberg equations using the Wannier interpolation technique as implemented in the EPW code [38–40]. To construct Wannier functions and phonon calculations, we have used a dense 30×30×1 k- and q-point mesh, respectively. A total of five maximally localized Wannier functions were constructed for the ML-LiBC. Fine 300×300×1 k- and 150×150×1 q-meshes for the electron and phonon, respectively, were used for interpolating EPC constants.

Figure 3 shows the calculated phonon dispersion, phonon DOS, anisotropic Eliashberg spectral function $\alpha^2F(\omega)$, and in-plane bond-stretching phonon mode of ML-LiBC. Clearly, the ML-LiBC is dynamically stable as there are no imaginary phonon frequencies. The optical phonons have rather flat dispersion near zone center and along the M-K direction that results in many peaks in the phonon DOS. The in-plane bond-stretching phonon mode is doubly degenerate at zone center $\omega = 86.5$ meV. The calculated Eliashberg spectral function shows that the phonon corresponding to energy 86.5 meV contributes significantly to the el-ph coupling. The

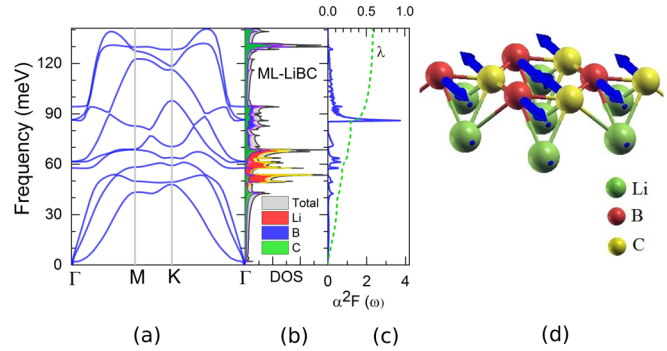

FIG. 3. (a) Phonon dispersions, (b) phonon density of states (DOS), (c) Eliashberg spectral function (d) In-plane bond stretching mode at zone center, for ML-LiBC.

overall isotropic el-ph coupling constant (λ) value is 0.59. However, our calculations show that el-ph coupling is highly anisotropic, even reaching 1.56 at some k-point of the BZ. The distributions of the λ over BZ for the first two bands (out of three partially occupied) are shown in Figs. 4(a) and 4(b), and for the third band, this distribution is like that of

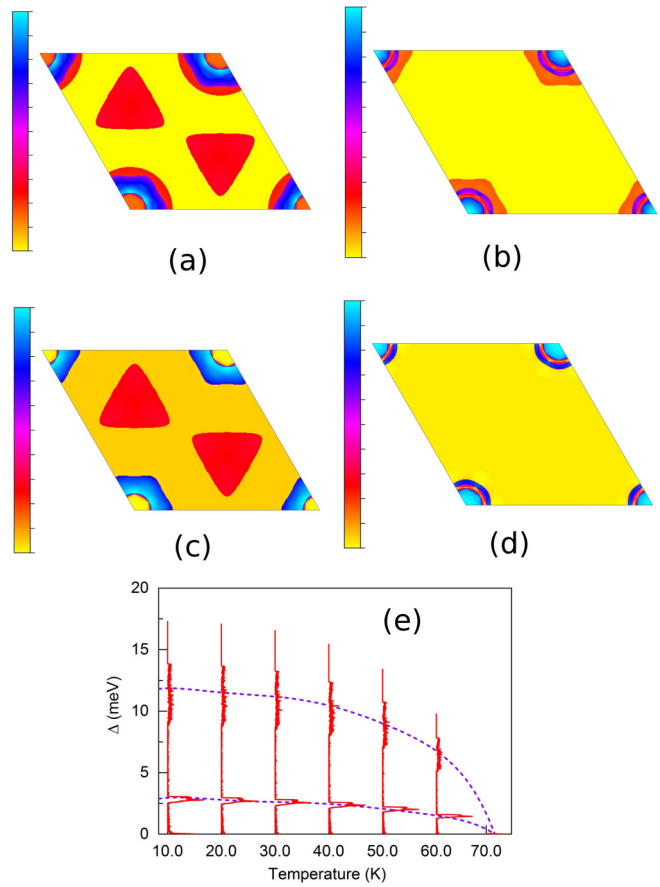

FIG. 4. Superconducting properties of ML-LiBC at 10 K. (a) and (b) Distribution of el-ph coupling constant, (in ranges of 0–1.21 and 0–1.56, respectively). (c) and (d) Distribution of superconducting gaps, (in ranges of 0–12.2 and 0–13.8 meV, respectively) over the first Brillouin zone (BZ) for the first two metallic bands. (e) Temperature evolution of superconducting gaps.

the second band. For the first band [Fig. 4(a)], λ varies from 0.00 to 1.21, and states around *K* point of BZ have weaker couplings, whereas states slightly away from the Γ point have the strongest couplings. In the case of other bands [Fig. 4(b)], λ varies from 0.00 to 1.56, and states close to the Γ point have the strongest coupling.

Another striking feature of this system is the existence of two-gap superconductivity, contrary to the ML of MgB_2, which is a three-gap superconductor [26]. Averaged values of superconducting gaps are 2.9 and 12.9 meV at 10 K. Figures 4(c) and 4(d) show the superconducting gap distributions for the first two bands, respectively, over the first BZ at 10 K. The third band gives a distribution like that of the second band. It is clear from Fig. 4(c) that the Fermi sheet around the *K* point, i.e., π sheet, hosts a smaller superconducting gap in the range of 2.4–3.0 meV, whereas the remaining three Fermi sheets around the Γ point [see Figs. 4(c) and 4(d)] host the largest superconducting gaps in the range of 9.5–13.8 meV. Figure 4(e) represents the temperature evolution of the superconducting gaps, and we notice that the two gaps are distinguishable at least up to 65 K, very close to $T_C \approx 70$ K. Dotted lines are guide to the eyes. In these calculations, the Coulomb repulsion parameter (μ^*) between two Cooper paired electrons is taken as 0.10, which is a reasonable choice for the *sp*-type covalent superconductor [41]. We also solved fully anisotropic Migdal-Eliashberg equations for $\mu^* = 0.13$, and the results show that the superconducting transition temperature reduces to 65 K.

To ascertain that ML-LiBC superconductivity is not perturbed by the Rashba effect [42], we calculated electronic band structure including SO interactions (Fig. S1 in the Supplemental Material [43]). Based on this set of calculations, we infer an extremely weaker SO splitting of bands in proximity to the Fermi level [43], and hence, the Rashba effect will not be detrimental for this system. In addition, our noncollinear spin-polarized and fixed spin-moment calculations clearly establish a nonmagnetic ground state for this system (Fig. S2 in the Supplemental Material [43]). Thus, these results further strengthen our predictions of high-T_C in ML-LiBC.

To study the effect of hydrogen on ML-LiBC, we placed one hydrogen atom above the B atom. Comparison of its electronic band structures [Fig. 5(a)] with a bare pristine ML exhibits a downward-shifted bonding π band with respect to E_F; as a result, the hole pocket around the *K* point vanishes. The dispersive band, originating from the hybridization of Li *s* and antibonding π states, also moves downward, intersecting E_F near *M* and *K* points along the Γ-*M* and Γ-*K* directions, respectively. As a result of this, now two bands cross E_F, leading to three Γ-centered Fermi sheets [Fig. 5(b)]. The DOS at the E_F also increases due to the flatness of the first band along the *M*-*K* direction. By solving full anisotropic Migdal-Eliashberg equations for $\mu^* = 0.13$, we find that the maximum value of the *el*-*ph* coupling reaches 2.89. In this

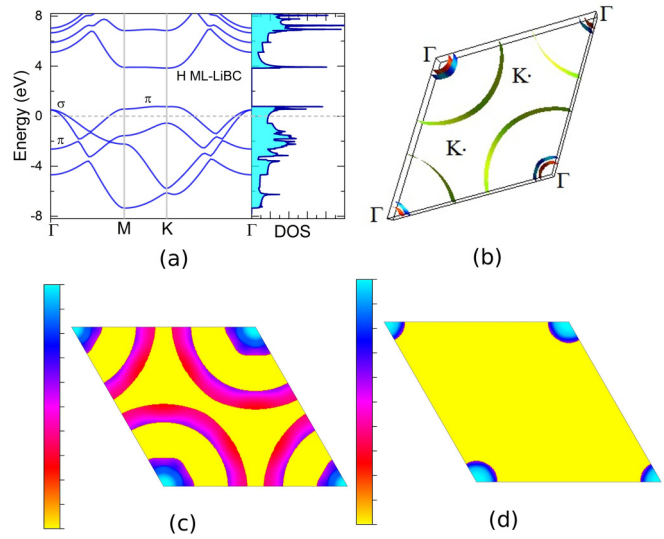

FIG. 5. (a) Electronic band structure and density of states (DOS; in units of states/eV/cell). (b) Fermi surface in first Brillouin zone (BZ). (c) and (d) Distribution of *el*-*ph* coupling constant in first BZ for both partially occupied bands (in the range of 0–2.89) for hydrogenated ML-LiBC at 10 K.

case also, the states close to the Γ point are strongly coupled to the in-plane bond-stretching phonon modes [see Figs. 5(c) and 5(d)]. Distribution of the superconducting gaps at 10 K over different Fermi sheets corresponding to two partially occupied bands also shows similar distributions as that of the *el*-*ph* coupling constant and thus is not shown here. Now the highest value of the superconducting gap on the σ sheet is 16.6 meV, and that for the π^* sheet is 5.5 meV at 10 K. Therefore, hydrogenated ML-LiBC is also a two-gap superconductor with Fermi surface averaged gaps of 5.20 and 16.28 meV at 10 K. The superconducting transition temperature increases to 80 K in this case.

In summary, we show that LiBC becomes a good metal in ML form, and it exhibits superconductivity at $T_C \approx 70$ K. A change of bonding character in the B-C honeycomb layer, due to the insufficient charge transfer from the Li atom, is attributed to the metallic nature of this system. It is worth mentioning that the observation of a superconducting gap opening at ∼30 K, in six-layer-thick MgB_2, by angle-resolved photoemission spectroscopy measurements [44] is consistent with the predictions of 20 K superconductivity in a pristine ML of MgB_2. We expect these findings will advance the existing knowledge of superconducting materials, and it will provide a better understanding for the design and development of 2D superconductors. We believe that our results will motivate experimentalists to explore 2D systems like ML-LiBC together with other layered materials for high-T_C superconductors at room pressure.

[1] H. K. Onnes, Commun. Phys. Lab. Univ. Leiden **133–144**, 37 (1913).

[2] J. Bednorz and K. Mueller, Zeit. Phys. B **64**, 189 (1986).

[3] M. K. Wu, J. R. Ashburn, C. J. Torng, P. H. Hor, R. L. Meng, L. Gao, Z. J. Huang, Y. Q. Wang, and C. W. Chu, Phys. Rev. Lett. **58**, 908 (1987).

[4] A. Schilling, M. Cantoni, J. D. Guo, and H. R. Ott, Nature **363**, 56 (1993).

[5] J. Bardeen, L. N. Cooper, and J. R. Schrieffer, Phys. Rev. **108**, 1175 (1957).

[6] J. Muller, Rep. Prog. Phys. **43**, 641 (1980).

[7] J. Nagamatsu, N. Nakagawa, T. Muranaka, Y. Zenitani, and J. Akimitsu, Nature **410**, 63 (2001).

[8] A. P. Drozdov, M. I. Eremets, I. A. Troyan, V. Ksenofontov, and S. I. Shylin, Nature **525**, 73 (2015).

[9] A. P. Drozdov, P. P. Kong, V. S. Minkov, S. P. Besedin, M. A. Kuzovnikov, S. Mozaffari, L. Balicas, F. F. Balakirev, D. E. Graf, V. B. Prakapenka, E. Greenberg, D. A. Knyazev, M. Tkacz, and M. I. Eremets, Nature **569**, 528 (2019).

[10] M. Somayazulu, M. Ahart, A. K. Mishra, Z. M. Geballe, M. Baldini, Y. Meng, V. V. Struzhkin, and R. J. Hemley, Phys. Rev. Lett. **122**, 027001 (2019).

[11] A. K. Verma, P. Modak, F. Schrodi, A. Aperis, and P. M. Oppeneer, Phys. Rev. B **103**, 094505 (2021).

[12] M. Wörle, R. Nesper, G. Mair, M. Schwarz, and H. G. Vonschnering, Z. Anorg. Allg. Chem. **621**, 1153 (1995).

[13] P. F. Karimov, N. A. Skorikov, E. Z. Kurmaev, L. D. Finkelstein, S. Leitch, J. MacNaughton, A. Moewes, and T. Mori, J. Phys.: Condens. Matter **16**, 5137 (2004).

[14] H. Rosner, A. Kitaigorodsky, and W. E. Pickett, Phys. Rev. Lett. **88**, 127001 (2002).

[15] A. K. Verma, P. Modak, D. M. Gaitonde, R. S. Rao, B. K. Godwal, and L. C. Gupta, Europhys. Lett. **63**, 743 (2003).

[16] T. Bazhirov, Y. Sakai, S. Saito, and M. L. Cohen, Phys. Rev. B **89**, 045136 (2014).

[17] M. Gao, Z.-Y. Liu, and T. Xiang, Phys. Rev. B **91**, 045132 (2015).

[18] Q. Li, X. Yan, M. Gao, and J. Wang, Europhys. Lett. **122**, 47001 (2018).

[19] M. Gao, X. Yan, Z.-Y. Liu, and X. Tiang, Phys. Rev. B **101**, 094501 (2020).

[20] A. M. Fogg, J. Meldrum, G. R. Darling, J. B. Claridge, and M. J. Rosseinsky, J. Am. Chem. Soc. **128**, 10043 (2006).

[21] A. Lazicki, C.-S. Yoo, H. Cynn, W. J. Evans, W. E. Pickett, J. Olamit, K. Liu, and Y. Ohishi, Phys. Rev. B **75**, 054507 (2007).

[22] M. Zhang, Europhys. Lett. **114**, 16001 (2016).

[23] M. Yamada, T. Hirahara, and S. Hasegawa, Phys. Rev. Lett. **110**, 237001 (2013).

[24] Y. J. Zhang, M. Yoshida, R. Suzuki, and Y. Iwasa, 2D Mater. **2**, 044004 (2015).

[25] K. Kanetani, K. Sugawara, T. Sato, R. Shimizu, K. Iwaya, T. Hitosugi, and T. Takahashi, Proc. Natl. Acad. Sci. **109**, 19610 (2012).

[26] J. Bekaert, A. Aperis, B. Partoens, P. M. Oppeneer, and M. V. Milošević, Phys. Rev. B **96**, 094510 (2017).

[27] P. C. Hohenberg, Phys. Rev. **158**, 383 (1967).

[28] N. D. Mermin and H. Wagner, Phys. Rev. Lett. **17**, 1133 (1966).

[29] T. Uchihasi, Supercond. Sci. Technol. **30**, 013002 (2017).

[30] T. Golod, A. Iovan, and V. M. Krasnov, Nat. Commun. **6**, 8628 (2015).

[31] J. N. Coleman *et al.*, Science **331**, 568 (2011).

[32] R. Ramirez, R. Nesper, H. G. von Schnering, and M. C. Böhm, Z. Naturforsch. A **42**, 670 (1987).

[33] P. Giannozzi *et al.*, J. Phys.: Condens. Matter **21**, 395502 (2009).

[34] J. C. Slater and G. F. Koster, Phys. Rev. **94**, 1498 (1954).

[35] R. F. W. Bader, *Atoms in Molecules: A Quantum Theory* (Oxford University Press, Oxford, 1990).

[36] P. Modak, R. S. Rao, B. K. Godwal, and S. K. Sikka, Pramana **58**, 881 (2002).

[37] S. Baroni, S. de Gironcoli, A. D. Corso, and P. Giannozzi, Rev. Mod. Phys. **73**, 515 (2001).

[38] A. Mostofi, J. R. Yates, G. Pizzi, Y.-S. Lee, I. Souza, D. Vanderbilt, and N. Marzari, Comput. Phys. Commun. **185**, 2309 (2014).

[39] F. Giustino, M. L. Cohen, and S. G. Louie, Phys. Rev. B **76**, 165108 (2007).

[40] S. Poncé, E. R. Margine, C. Verdi, and F. Giustino, Comput. Phys. Commun. **209**, 116 (2016).

[41] G. Profeta, M. Calandra, and F. Mauri, Nat. Phys. **8**, 131 (2012).

[42] Y. A. Bychkov and E. I. Rashba, JETP Lett. **39**, 78 (1984).

[43] See Supplemental Material at http://link.aps.org/supplemental/10.1103/PhysRevB.104.054504 for details on Rashba effect and magnetic calculations.

[44] J. Bekaert, L. Bignardi, A. Aperis, P. van Abswoude, C. Mattevi, S. Gorovikov, L. Petaccia, A. Goldoni, B. Partoens, P. M. Oppeneer, F. M. Peeters, M. V. Milosevic, P. Rudolf, and C. Cepek, Sci. Rep. **7**, 14458 (2017).